

AN ITERATIVE METHOD FOR DEDUCING TROPOSPHERIC TEMPERATURE AND MOISTURE PROFILES FROM SATELLITE RADIATION MEASUREMENTS

WILLIAM L. SMITH

National Environmental Satellite Center, ESSA, Washington, D.C.

ABSTRACT

An iterative method for deducing the general temperature and moisture structure of the troposphere from satellite radiation measurements of medium spectral resolution is described. The temperature and moisture profiles derived from simulated and radiometrically observed radiances, pertaining to clear atmospheres, are shown to agree favorably with the radiosonde profiles. The method is expanded to enable the inference of the temperature and moisture profiles of partly cloudy atmospheres. The ability of the method to recognize severe noise in radiance observations which lead to unacceptable temperature and moisture solutions is demonstrated.

1. INTRODUCTION

Since the inception of the meteorological satellite, much attention has been directed toward the problem of inferring the temperature structure of the atmosphere from infrared radiation observations taken from orbiting vehicles. Unfortunately, no unique closed-form solution for the temperature profile can be obtained from a finite number of remote radiation measurements. Nevertheless, numerous approximate solutions derived from high spectral resolution radiance measurements in the 15μ CO_2 band may be found in the literature (e.g., Wark [1], Yamamoto [2], King [3], Wark and Fleming [4]). All of the solutions obtained to date, however, have been directed toward deducing the temperature profile of the atmosphere above the 500-mb. level where the dependence of the sensed radiation on water vapor may be neglected. Furthermore, none of the solutions given in the literature to date is directly applicable when partial cloudiness exists within the field of view of the radiometer.

In this paper a predictor-corrector method, which makes use of five remote medium spectral resolution measurements, is utilized to deduce the temperature and moisture structure of the non-overcast troposphere. The solutions obtained by this method are shown to be adequate to describe the significant qualities of the troposphere. A relation between severe noise in the radiance observations which leads to unacceptable temperature and moisture solutions and the number of iterations required to obtain these solutions is also demonstrated.

2. THEORETICAL BASIS

The intensity of the radiation reaching a satellite detector at the frequency ν may be expressed for a clear atmosphere as

$$I(\nu) = B[\nu, T(p_0)]\tau[\nu, U(p_0)] - \int_0^{p_0} B[\nu, T(p)] \frac{\partial \tau[\nu, U(p)]}{\partial p} dp \quad (1)$$

where $B[\nu, T(p)]$ is the Planck radiance which is a function of the temperature T at the pressure p ; $\tau[\nu, U(p)]$ is the transmissivity of the mass of optically active gas U above the pressure p ; and p_0 refers to the pressure at the earth's surface. The first term on the right in (1) represents the surface contribution while the second term illustrates the atmospheric contribution to the total radiation. Thus, if the distribution of absorbing gas is known, the radiation measured by the satellite can be related to the temperature profile; or conversely, if the temperature profile is known the intensity of radiation can be related to the distribution of absorbing gas. Furthermore, the transmittance function is highly dependent on frequency as well as gas amount. Near absorbing band centers only a small amount of absorbing gas is necessary to completely hinder transmission; hence, most of the outgoing radiation at frequencies near band centers arises from the upper levels of the atmosphere. On the other hand, at frequencies far from absorbing band centers relatively large amounts of absorbing gas are necessary to hinder transmission; hence, at these frequencies most of the radiation leaving the atmosphere arises from the lower layers of the atmosphere. It is this relationship which enables vertical resolution of the temperature and absorbing gas profiles to be obtained from a set of radiation measurements in different frequency regions. In this paper radiation measurements in the wings of the 15μ CO_2 band are used to derive the temperature profile of the troposphere since the distribution of CO_2 is known. However, because there is significant absorption in these spectral regions by the water vapor existing in the troposphere, a simultaneous solution for the

water vapor distribution must be obtained in order to arrive at an acceptable solution for the temperature profile. Measurements in the rotational and 6.3μ bands of water vapor are utilized to deduce a simultaneous estimate of the water vapor distribution of the troposphere.

3. METHOD OF INFERENCE

The temperature distribution of the troposphere may be represented adequately by two lapse rates, $\gamma = -\partial T/\partial z$: one pertaining to the lowest 50 mb. of atmosphere, γ_1 , and one pertaining to the atmosphere above the lowest 50 mb., γ_2 . Assuming hydrostatic equilibrium these distributions are given by

$$T(p) = T(p_0) \left(\frac{p}{p_0} \right)^{\frac{\gamma_1 R}{g}}, \quad p_0 - 50 \leq p \leq p_0 \quad (2)$$

and

$$T(p) = T(p_0 - 50) \left(\frac{p}{p_0 - 50} \right)^{\frac{\gamma_2 R}{g}}, \quad p_t \leq p \leq p_0 - 50 \quad (3)$$

where R is the gas constant for dry air, g is the gravitational acceleration, and p_t refers to the tropopause pressure. The average vertical distribution of specific humidity, $w(p)$, for the troposphere is also assumed to be adequately represented by a power law:

$$w(p) = w(p_0) \left(\frac{p}{p_0} \right)^\lambda, \quad p_t \leq p \leq p_0 \quad (4)$$

where λ is a dimensionless parameter describing the moisture lapse with pressure. If the temperature of the level 50 mb. above the surface exceeds the surface temperature by more than 5°C ., a better approximation to the moisture distribution of the lowest 50 mb. can be made by assuming the relative humidity of this region to be constant. In this case the specific humidity of the lowest 50 mb. is given by

$$w(p) = \frac{w(p_0)}{w_s[T(p_0)]} w_s[T(p)], \quad p_0 - 50 \leq p \leq p_0. \quad (5)$$

The distribution above the lowest 50 mb. is then assumed to be given by

$$w(p) = w(p_0 - 50) \left(\frac{p}{p_0 - 50} \right)^\lambda, \quad p_t \leq p \leq p_0 - 50. \quad (6)$$

Thus, the tropospheric distributions of temperature and moisture may be assumed to be described by the five parameters $T(p_0)$, γ_1 , γ_2 , $w(p_0)$, and λ . It is the purpose of this paper to estimate these parameters from satellite radiation observations.

Figure 1 illustrates the relative contributions to the outgoing radiation in five different spectral intervals. This figure is based on the temperature distribution of the A.R.D.C. Standard Atmosphere and a water vapor dis-

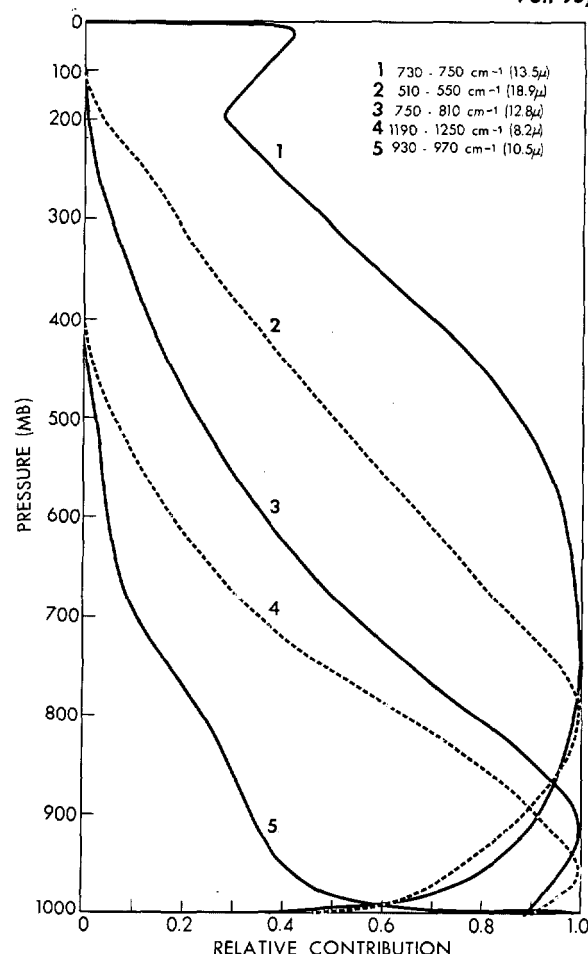


FIGURE 1.—Relative contribution to the outgoing radiance in five spectral intervals. These curves reveal the atmospheric layers upon which the measured outgoing radiance is most heavily dependent.

tribution characterized by equation (4) with $w(p_0) = 5.2 \text{ gm./kg.}$ and $\lambda = 2.5$. Curves 1 and 3 pertain to outgoing radiation in two different spectral regions of the 15μ band where water vapor absorption is at a minimum. As may be inferred from their respective relative contributions, the outgoing radiation in these two regions is highly dependent on the temperature lapse rates of the middle and lower troposphere. Curve 2 refers to a spectral region of the rotational water vapor band where the outgoing radiation is highly dependent on the distribution of moisture throughout the troposphere. Curve 4 refers to a spectral region in a wing of the 6.3μ band where the outgoing radiation is highly dependent on the moisture near the earth's surface, whereas Curve 5 refers to a spectral region in the 10μ water vapor window region where the outgoing radiation from clear atmospheres is mainly dependent on the surface temperature. (All radiation calculations in this paper are based on the generalized absorption coefficients given by Möller and Raschke [5]. The $15\mu \text{ CO}_2$ spectral intervals employed here were selected because of the good agreement between the average transmis-

sivities computed, for each spectral interval, from these absorption coefficients and the average transmissivities obtained from the high spectral resolution observations of Burch et al. [6].)

As illustrated above, the outgoing radiation in each of the spectral intervals referred to in figure 1 may be physically related to one of the temperature and moisture parameters of the model profiles given by equations (2) to (6). Knowing this physical relation, we may utilize a predictor-corrector method to solve for the five parameters of the model profiles from observations of the outgoing radiation in the five spectral intervals. Basically this method consists of reducing the intensity residuals by systematically varying the parameters of the model profiles. The procedure begins with an initial estimate of the five parameters in which few, if any, of the observed radiances are satisfied within a preset convergence criterion. In practice, the convergence criterion is chosen as the random error of the instrument. The surface temperature is then varied until the computed radiance in the 10.5μ region agrees with the observed radiance in this spectral region. With a first estimate of surface temperature, the upper tropospheric lapse rate, γ_2 , is varied until the computed radiance in the 13.5μ region agrees with its observed value. Having changed the upper tropospheric lapse rate from its initial condition, one must then obtain another estimate of the surface temperature and subsequently further estimates of the upper-level lapse rate until finally both the 10.5μ and 13.5μ radiances are satisfied by the same values of surface temperature and upper tropospheric lapse rates. The procedure continues in a similar manner iterating next on surface specific humidity using the 8.2μ radiance and then on the specific humidity lapse rate utilizing the 18.9μ radiance and subsequently on the lower tropospheric lapse rate using the observed 12.8μ radiance until finally five parameters of the model profiles result which satisfy all five satellite radiance measurements within the observational error. The resulting model profiles of temperature and moisture are then assumed to represent the actual temperature and moisture distribution within the atmosphere beneath the satellite. The details of the above procedure are given by Smith [7].

The outgoing radiation in the 13.5μ region is slightly dependent on the temperature distribution of the stratosphere. However, since this contribution above the troposphere is less than 3 percent of the total outgoing energy, little error will result by assuming the temperature distribution of the A.R.D.C. Standard Atmosphere for this region. Also it is known that the surface specific humidity must lie between zero and its saturation value. In the above-described procedure if a calculated surface specific humidity exceeds its calculated saturation value, the surface humidity is temporarily assumed to be nine-tenths of its saturation value. If the calculated specific humidity is equal to or less than zero, it is temporarily

assumed to be three-tenths of its saturation value. This procedure allows the iterative process to be continued in a physically consistent manner.

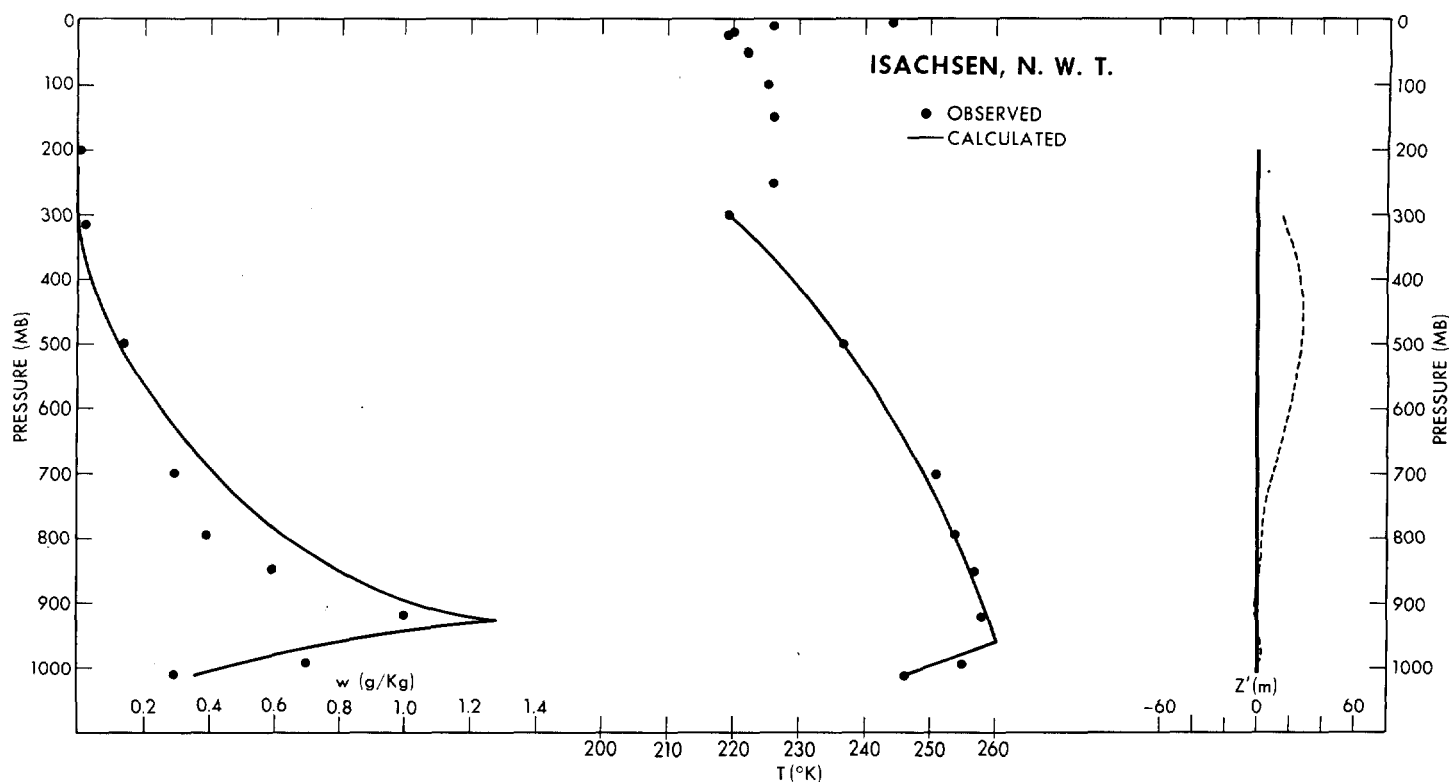
4. RESULTS

Figure 2 illustrates the temperature and moisture solutions derived from the same initial conditions for two entirely different types of cloudless soundings. The temperature and moisture calculations in the upper illustration were made from exact outgoing radiance values computed from the radiosonde temperature and moisture profiles. The dots represent the radiosonde measurements whereas the solid curves represent the temperature and moisture profiles calculated from the radiance values. In this case, the largest errors in the calculated temperature and specific humidity are less than 2° K. and 0.2 gm./kg., respectively. The dashed curve in figure 2a illustrates the difference in the heights of the various pressure levels obtained from the observed surface pressure and the radiosonde and calculated temperature soundings. The errors in the heights are less than 40 m. throughout the troposphere.

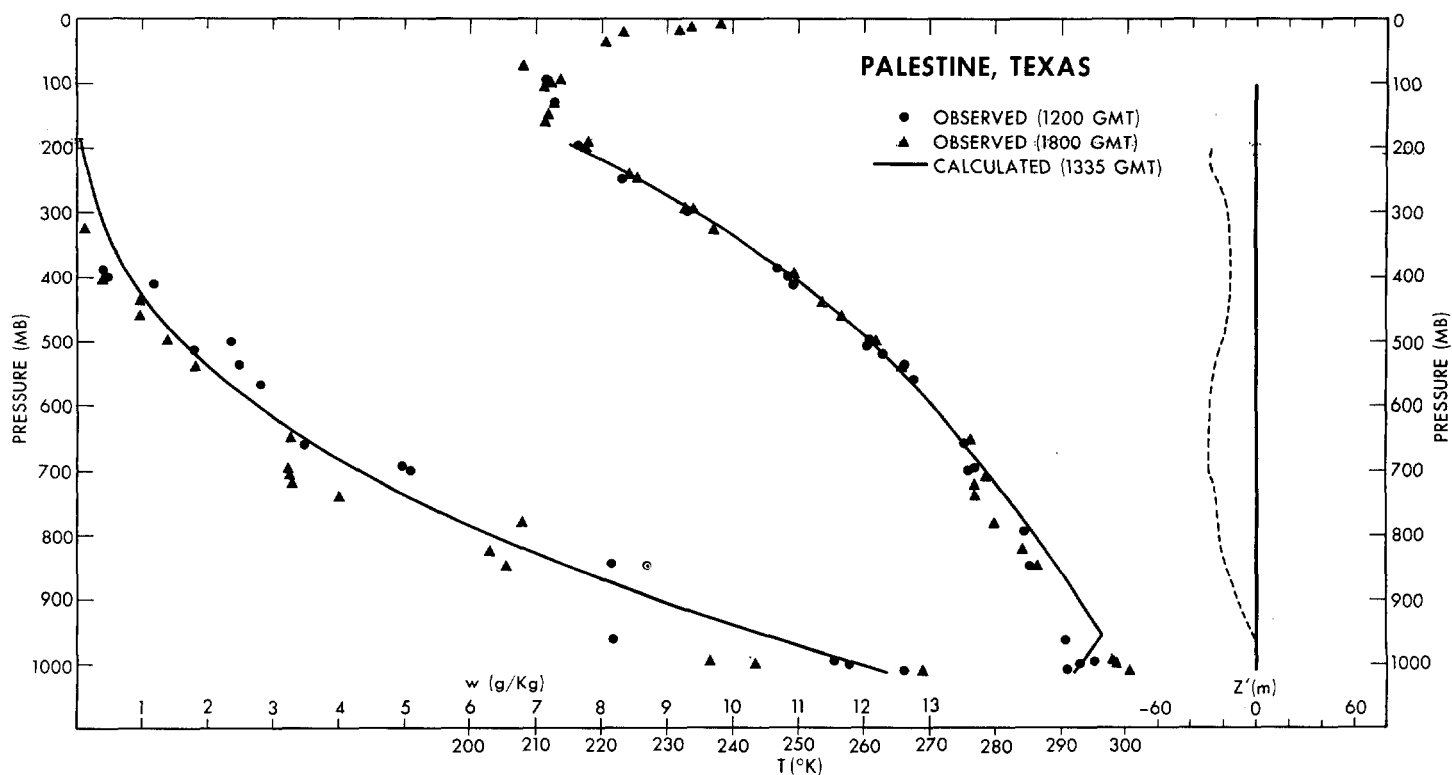
Figure 2b illustrates the temperature and moisture solutions derived from radiance observations taken by a NASA interferometer which was positioned on a balloon at the 7-mb. level over Palestine, Tex., on May 8, 1966. This interferometer flight is described elsewhere by Chaney, Drayson, and Young [8]. The interferometer measured the upward radiances in the spectral region between 500 cm^{-1} and 2000 cm^{-1} with a spectral resolution of approximately 5 cm^{-1} . From a three-scan average spectrum of upward radiance, the total radiance of each spectral region employed in this paper was computed and subsequently the temperature and moisture profiles shown in figure 2b were calculated. The radiosonde and calculated profiles are in good agreement; the only substantial disagreement occurring in the lowest 200 mb. As can be seen from the height deviation curve, however, errors in temperature occurring near the earth's surface will not lead to a substantial error in the heights of pressure levels of the middle and upper troposphere. This is due to the fact that an error in the height, z' , of a pressure level p above the earth's surface is given by

$$z' = \frac{R}{g} \int_p^{p_0} T'(p) d \ln p \quad (7)$$

where $T'(p)$ is the temperature error. Hence, because of its dependence on the natural logarithm of pressure, a given temperature error will lead to a greater error in z if it occurs near the level p than if it occurs near the surface p_0 . It is also apparent from equation (7) that it is necessary to know, to a high degree of accuracy, the surface pressure p_0 in order to derive a useful estimate of z . Unfortunately an accurate estimate of p_0 cannot be obtained from satellite radiation measurements.



(a.)



(b.)

FIGURE 2.—Solutions of temperature and moisture for two clear-sky situations. The dots and triangles represent radiosonde values and the solid lines the calculated profiles. The dashed curve at the right illustrates the differences between the heights of various pressure levels in meters as calculated from the radiosonde-observed and radiance-calculated temperature soundings (i.e., $z' = z$ (radiosonde) $- z$ (calculated)).

5. METHOD OF SOLUTION IN THE PRESENCE OF CLOUDS

Since clouds tend to be opaque to infrared radiation, solutions for the temperature and moisture of the lower troposphere can be obtained only from radiances leaving relatively clear atmospheric columns. Furthermore, the solution for the temperature and moisture profiles above non-opaque clouds can be obtained only if the heights, amounts, and opacities of the clouds are known. Hence it is desirable, if not necessary, to utilize only measurements of the infrared radiances leaving clear atmospheric columns to deduce the structure of the troposphere.

It is apparent that a near global network of observations of the infrared radiances leaving clear atmospheric columns can be provided only by a satellite radiometer of high geometrical resolution. The high geometrical resolution is necessary to observe the radiances propagating through any clear columns which may exist in the relatively cloudy regions of the globe. An objective method of deducing the clear-column radiances from a field of measurements taken over an atmosphere composed of broken clouds is described below.

Consider a field of radiation measurements as might be provided by a radiometer scanning a region of atmosphere composed of broken clouds. If the angular resolution of the scanning radiometer is sufficiently high, the measured radiances composing the field will propagate from either cloud-covered or cloudless columns. The amount of cloudiness, N , in the region of the observations is given by

$$N = \frac{n}{n+m} \quad (8)$$

where n is the number of cloud-covered columns and m is the number of clear columns. Now the average of all the radiances, at a given frequency, measured in the field is given by

$$\bar{I}(\nu) = \frac{1}{n+m} \sum_{i=1}^{n+m} I_i(\nu) = \frac{1}{n+m} \sum_{i=1}^n I_{CD}^i(\nu) + \frac{1}{n+m} \sum_{i=1}^m I_{CLR}^i(\nu) \quad (9)$$

where $I_{CD}^i(\nu)$ and $I_{CLR}^i(\nu)$ represent radiances measured over cloud-covered and cloudless columns, respectively. Since the mean radiances for the cloud-covered and cloudless columns are given by

$$\bar{I}_{CD}(\nu) = \frac{1}{n} \sum_{i=1}^n I_{CD}^i(\nu) \quad (10)$$

and

$$\bar{I}_{CLR}(\nu) = \frac{1}{m} \sum_{i=1}^m I_{CLR}^i(\nu), \quad (11)$$

respectively, equation (9) may be written utilizing (8) as

$$\bar{I}(\nu) = N\bar{I}_{CD}(\nu) + (1-N)\bar{I}_{CLR}(\nu). \quad (12)$$

If the average radiance arising from the cloud-covered columns and the amount of cloudiness in the region are

known, the average radiance leaving the cloudless columns may be determined, by equation (12), from the average of all the observed intensities in the region. In practice, however, it is impossible to obtain only radiances arising from completely cloudless and cloud-covered columns since a radiometer of finite resolution may often view columns which are only partially cloudy. It is then necessary to consider an analog to (12)

$$\bar{I}(\nu) = N^* I^*(\nu) + (1-N^*) \bar{I}_{CLR}(\nu) \quad (13)$$

where $I^*(\nu)$ is an "effective" cloud column radiance and N^* is an "effective" cloud amount. Since N must range between zero (cloudless) and one (overcast), it may be assumed that N^* also ranges between zero and one. Under this assumption $I^*(\nu)$ is defined as

$$I^*(\nu) = \frac{1}{k} \sum_{i=1}^{n+m} I_i^*(\nu)$$

where

$$I_i^*(\nu) = \begin{cases} I_i(\nu), & I_i \leq \bar{I}(\nu) \\ 0, & I_i > \bar{I}(\nu) \end{cases} \quad (14)$$

and k equals the number of non-zero $I_i^*(\nu)$ values, to insure that (13) is always satisfied in the limiting case $N^*=1$ (i.e., complete overcast). Since $\bar{I}(\nu)$ and $I^*(\nu)$ may be obtained from the field of observations, the average clear column radiance may be obtained from (13), rewritten in the form

$$\bar{I}_{CLR}(\nu) = \frac{\bar{I}(\nu) - N^* I^*(\nu)}{(1-N^*)} \quad (15)$$

if N^* is known. From independent observations of the surface temperature and water vapor mixing ratio, a good initial estimate of the average radiance leaving the clear columns in the "window" region of the spectrum, $\hat{I}_{CLR}(W)$, may be made. An estimate of N^* for the window region may then be calculated from equation (13), written in the form

$$\hat{N}^* = \frac{\bar{I}(W) - \hat{I}_{CLR}(W)}{I^*(W) - \hat{I}_{CLR}(W)} \quad (16)$$

where W refers to the window frequency interval (i.e., 930–970 cm^{-1}) and the quantities with the circumflex refer to estimated values. If we assume that N^* is not frequency dependent, the value obtained in equation (16) may then be utilized in (15) to provide estimates of $\bar{I}_{CLR}(\nu)$ for the remaining spectral intervals which subsequently may be utilized to estimate the average temperature and moisture lapse rates pertaining to the total area scanned by the radiometer.

The complete procedure for deducing the average temperature and moisture profiles from a field of measurements over an atmosphere consisting of broken clouds may now be summarized as follows:

(1) From the field of radiation observations the mean quantities $\bar{I}(\nu)$ and $I^*(\nu)$ are calculated for each spectral interval.

(2) From independent observations of surface temperature and mixing ratio and from initial estimates of the model parameters γ_1 , γ_2 , and λ , an initial estimate of clear-column intensity pertaining to the window spectral region, $\hat{I}_{CLR}(W)$, is obtained from equation (1).

(3) From equations (16) and (15) initial estimates are made for the intensities propagating from the clear columns in the 730–750-cm.⁻¹, 750–810-cm.⁻¹ and 510–550-cm.⁻¹ intervals.

(4) The same numerical predictor method described earlier is then utilized to obtain first estimates of the model parameters γ_1 , γ_2 , and λ .

(5) With the first estimates of the γ_1 , γ_2 , and λ parameters obtained in step (4), second estimates of $\bar{I}_{CLR}(W)$, N^* , and $I_{CLR}(\nu)$ for the remaining spectral intervals are made which subsequently lead to second estimates of γ_1 , γ_2 , and λ . The procedure is repeated until the condition

$$\hat{N}_i^* - \hat{N}_{i-1}^* < 0.005$$

is satisfied.

Table 1 lists values of outgoing radiance (ergs/cm.² sec. strdn. cm.⁻¹) as a function of various cloud pressures, p_c , and effective emissivities, ϵ^* (defined as the product of cloud amount and cloud emissivity), as calculated from

TABLE 1.—Outgoing radiation (ergs/cm.² sec. strdn. cm.⁻¹), listed as a function of cloud pressure and effective cloud emissivity, calculated from the radiosonde temperature and moisture profiles shown in figure 3

p_c (mb.)	ϵ^*	$I(10.5\mu)$	$I(12.8\mu)$	$I(13.5\mu)$	$I(18.9\mu)$
370.....	1.00	*40.5	*60.3	*61.5	*84.0
370.....	0.50	*66.3	*86.5	*76.5	*101.0
750.....	1.00	81.3	104.2	88.5	116.8
750.....	0.50	86.8	108.3	90.0	117.3
1000.....	0	92.0	112.5	91.5	118.0
1000.....	0	92.0	112.5	91.5	118.0
Average radiation.....		76.5	97.4	83.3	109.2
Effective cloud radiation.....		53.4	73.4	69.0	92.5

*Denotes values less than the average and hence those values used to deduce the effective cloud radiation.

a radiosonde temperature and moisture profile at Brownsville, Tex. This set of radiances simulates a set which might have been observed by a high resolution radiometer which was scanning an area surrounding Brownsville when broken clouds existed at the 370 and 750-mb. levels. From this set of values the mean radiance, $\bar{I}(\nu)$, and effective cloud radiance, $I^*(\nu)$, were computed for each spectral interval. From these values and the observed values of surface temperature and surface mixing ratio, the temperature and moisture profiles were calculated by the procedure outlined above. Figure 3 compares the

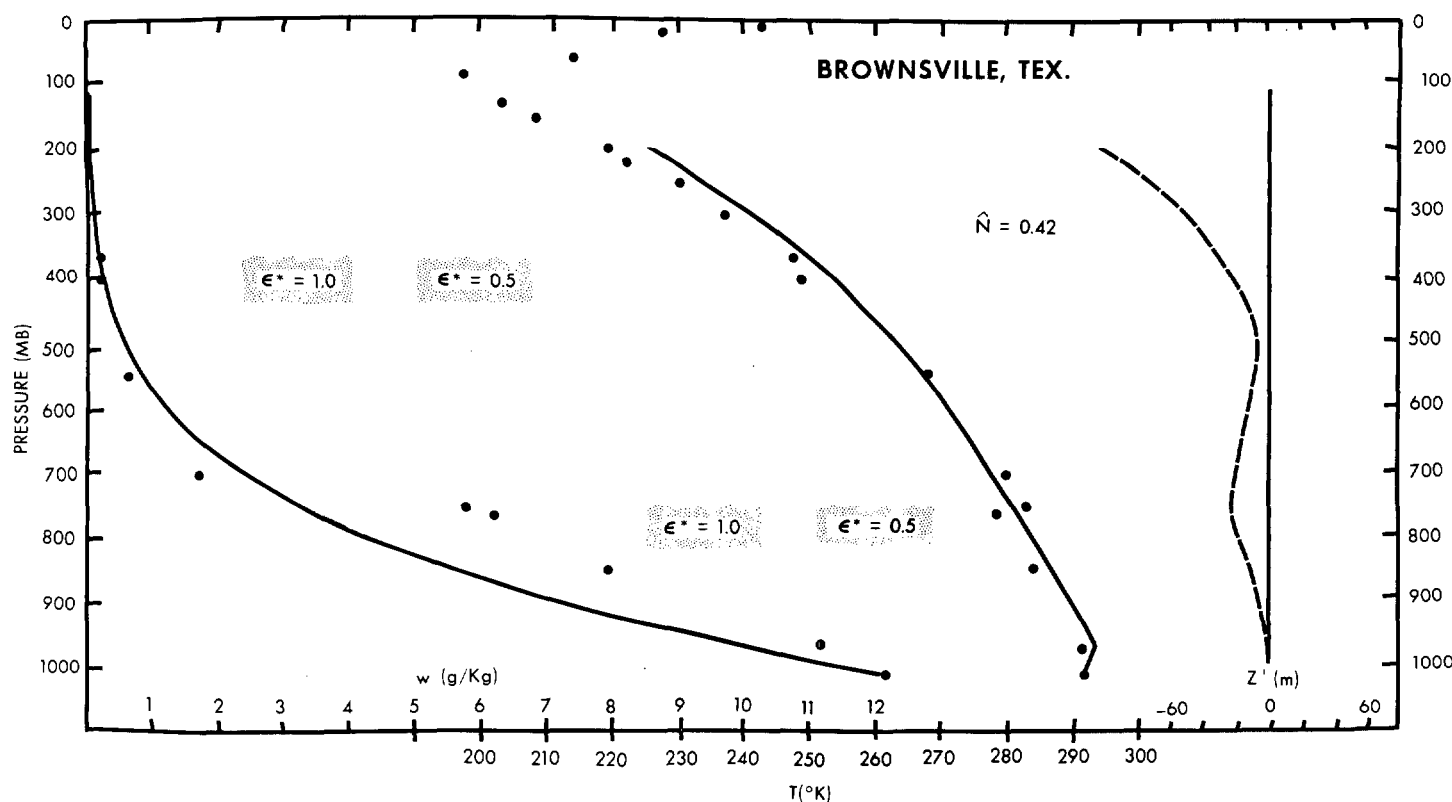


FIGURE 3.—Temperature and moisture solution derived from the radiances given in table 1.

radiosonde profiles with the calculated profiles. As shown, the solutions for the average temperature and moisture lapse rates are entirely satisfactory. For this case the effective cloud amount, N^* , converged to a value of 0.42.

The example given above illustrates the value of having radiation measurements of relatively high spatial resolution for determining temperature and moisture profiles in the atmosphere. The distinct advantage of this procedure is that it is not necessary to determine explicitly where any clouds are located or what percentage of cloud cover affects a single radiance measurement. It is required, however, that the set of data possess considerable information on the radiance propagating from any clear columns (i.e., $N^* < 1$). If the field of view of the satellite radiometer is relatively small, this requirement can be met under most types of broken cloud conditions.

6. INFLUENCE OF RANDOM ERRORS OF OBSERVATION

Random errors in the radiance measurements can lead to totally unacceptable solutions for the temperature and moisture profiles. The number of iterations necessary for convergence is directly related to random errors in the radiance measurements. To demonstrate this relationship 100 sets of random errors, distributed according to a normal distribution with a standard deviation of one-half percent of the true radiance, were introduced into the exact radiances calculated from the A.R.D.C. Standard Atmosphere. From these 100 sets of error radiances, 100 solutions for the temperature and moisture profiles were obtained. Table 2 lists the largest mean of the absolute value of the temperature errors which occurred in all the solutions requiring less than 200, 300, 450, and more than 450 iterations. About 55 percent of the solutions were essentially unaffected by the random errors, and approximately 96 percent of the solutions are physically acceptable. The remaining 4 percent which are totally unacceptable solutions can be readily detected from the extreme number of iterations required to arrive at these solutions. In the case of larger instrumental errors a similar relationship should be observed except that a much smaller number of deduced solutions could be utilized for meteorological purposes.

TABLE 2.—Largest mean temperature error vs. number of iterations

Number of iterations	Largest mean error ($^{\circ}$ K.)	Percent of total sample
<200	1.6	55
<300	3.6	96
<450	5.6	98
>450	17.3	100

7. CONCLUSION

It is felt that reliable estimates of the general temperature and moisture structure of the troposphere can be deduced from satellite radiation observations of relatively high spatial and medium spectral resolution. Although the type of radiation observations considered here have not yet been provided by meteorological satellites, it is hoped that similar measurements will be available in the near future. A study is currently being conducted to determine the optimum spectral characteristics of such measurements. These measurements should indeed be capable of filling the large gaps of meteorological information which presently exist over oceanic and other remote areas of the globe.

ACKNOWLEDGMENTS

The author is indebted to Professors Lyle Horn, Verner Suomi, and Donald R. Johnson of the University of Wisconsin, and Mr. H. E. Fleming and Dr. D. Q. Wark of the National Environmental Satellite Center for their helpful suggestions and criticisms. Special thanks are extended to Dr. R. A. Hanel of the National Aeronautics and Space Administration, and to Mr. Fred Bartman of the University of Michigan, who supplied the author with the Balloon Interferometer measurements prior to their publication.

REFERENCES

1. D. Q. Wark, "On Indirect Temperature Sounding of the Stratosphere from Satellites," *Journal of Geophysical Research*, vol. 66, No. 1, Jan. 1961, pp. 77-82.
2. G. Yamamoto, "Numerical Method for Estimating the Stratospheric Temperature Distribution from Satellite Measurements in the CO₂ Band," *Journal of Meteorology*, vol. 18, No. 5, Oct. 1961, pp. 581-588.
3. J. I. F. King, "Inversions by Slabs of Varying Thickness," *Journal of the Atmospheric Sciences*, vol. 21, No. 3, May 1964, pp. 324-326.
4. D. Q. Wark and H. E. Fleming, "Indirect Measurements of Atmospheric Temperature Profiles from Satellites," *Monthly Weather Review*, vol. 94, No. 6, June 1966, pp. 351-362.
5. F. Möller and E. Raschke, "Evaluation of TIROS III Radiation Data," Interim Report No. 1, National Aeronautics and Space Administration, July 1963, 114 pp.
6. D. E. Burch, D. Grvnak, and D. Williams, "Infrared Absorption by Carbon Dioxide," *Scientific Report No. 2*, contract AF19 (604)-2633, The Ohio State University Research Foundation, Columbus, Ohio, Jan. 1961.
7. W. L. Smith, "A Physical-Numerical Model for Deriving Tropospheric Structure from Satellite Radiation Measurements," Ph. D. Thesis, University of Wisconsin, August 1966.
8. L. W. Chaney, S. R. Drayson, and C. Young, "Fourier Transform Spectrometer-Radiative Measurements and Temperature Inversion," *Applied Optics*, vol. 6, No. 2, Feb. 1967.

[Received February 15, 1967; revised April 6, 1967]